727

A heteronuclear correlation experiment for simultaneous determination of ^{15}N longitudinal decay and chemical exchange rates of systems in slow equilibrium

Neil A. Farrow[a], Ouwen Zhang[a,b], Julie D. Forman-Kay[b] and Lewis E. Kay[a]

[a]Protein Engineering Network Centres of Excellence and Departments of Molecular and Medical Genetics, Biochemistry and Chemistry, University of Toronto, Toronto, ON, Canada M5S 1A8
[b]Division of Biochemistry Research, Hospital for Sick Children, 555 University Avenue, Toronto, ON, Canada M5G 1X8

SUMMARY

A heteronuclear correlation experiment is described which permits simultaneous characterization of both ^{15}N longitudinal decay rates and slow conformational exchange rates. Data pertaining to the exchange between folded and unfolded forms of an SH3 domain is used to illustrate the technique. Because the unfolded form of the molecule, on average, shows significantly higher NH exchange rates than the folded form, an approach which minimizes the degree of water saturation is employed, enabling the extraction of accurate rate constants.

NMR spectroscopy is a powerful tool for the measurement of rates of interconversion of chemical systems that are in slow dynamic equilibrium (Gutowsky and Saika, 1953; Forsen and Hoffman, 1963). One- and two-dimensional (1D, 2D) homonuclear exchange experiments have been successfully employed for studies of exchange processes in small molecules. However, due to spectral overlap, homonuclear approaches may not be practical when applied to macromolecules such as proteins. In addition, homonuclear methods such as NOESY (Macura and Ernst, 1980) or ROESY (Bothner-By et al., 1984; Bax and Davis, 1985) may be of limited utility when the exchange cross peaks are close to the diagonal peaks. To overcome this problem, an approach that exploits the increased chemical shift resolution of proton-detected heteronuclear correlation experiments has been proposed by Montelione and Wagner (1989). In one class of experiments, chemical exchange rates are measured by monitoring the exchange of two-spin heteronuclear order, I_zS_z, between different molecular conformations. A second class of experiments makes use of the net transfer of heteronuclear longitudinal magnetization to measure rates of interconversion. In both cases, the resultant spectra consist of 'auto' peaks for each conformation of a coupled I,S pair, plus 'exchange' peaks that arise due to magnetization transfer during a mixing

period. If the spectra are recorded under fully relaxed conditions and in the limit of zero mixing time, the relative volumes of the auto peaks of the different conformations may be used to characterize equilibrium constants. In addition, exchange rates may be determined from the initial slopes of buildup curves (derived from volumes of exchange peaks), obtained from spectra recorded using a series of mixing periods. More recently, Wider et al. (1991) have proposed a difference correlation experiment to facilitate the measurement of exchange rates from the exchange peaks in spectra with minimal interference from the auto peaks.

Our interest in developing accurate and sensitive methods for characterizing rates of exchange in a two-state exchanging system was stimulated by recent studies in our laboratories of a 59-residue fragment comprising the N-terminal SH3 domain of the protein drk. Studies have shown that this fragment exists in dynamic equilibrium between its native, folded form and an unfolded form, denoted by 'n' and 'u', respectively (Zhang and Forman-Kay, 1994). In this communication we present a 2D ^{1}H-^{15}N heteronuclear correlation experiment which permits the accurate measurement of both chemical exchange and longitudinal relaxation rates. The experiment is based on the transfer of longitudinal nitrogen magnetization, N_z, between exchanging conformers during the mixing time and is similar to an approach described by Montelione and Wagner (1989). Longitudinal relaxation and chemical exchange rates can be extracted by fitting theoretical exchange/decay curves to the measured data, as described below.

The pulse sequence used to simultaneously determine ^{15}N longitudinal decay and chemical exchange rates is shown in Fig. 1. The scheme is similar to experiments reported previously in the literature for the measurement of heteronuclear longitudinal relaxation times (Kay et al., 1989; Palmer et al., 1991a). Pulsed field gradients have been included in the experiment in order to aid in the suppression of artifacts and minimize the water signal (Bax and Pochapsky, 1992; John et al., 1992). In addition, the gradient g1, following the first ^{15}N 90° pulse, ensures that the detected signal arises solely from proton rather than from nitrogen magnetization. An important consideration in the design of this experiment is the fact that for many residues in the SH3 fragment, NH exchange with water is much more rapid in the unfolded form than in the folded conformation. Unless precautions are taken to minimize the saturation of water in the experiment, errors can occur in the measurement of both exchange and longitudinal relaxation rates. For example, consider the mixing time T, which includes ^{1}H 180° pulses to eliminate the effects of cross correlation between ^{1}H-^{15}N dipolar and ^{15}N CSA mechanisms (Boyd et al., 1990; Kay et al., 1992; Palmer et al., 1992). Unless care is taken to ensure that these pulses do not perturb the water resonance, water saturation will become more pronounced as a function of increasing T. Because magnetization originates on the NH proton in these experiments and exchange with water is more prevalent in the unfolded form, a preferential decrease in the intensity of the peaks associated with the unfolded form of the protein will occur as a function of increasing values of T. This will result in an artificial increase in measured relaxation rates.

In order to minimize water saturation, an approach using selective pulses on the water resonance has been employed (Grzesiek and Bax, 1993a; Kay et al., 1994). For example, at point a in the sequence the magnetization of interest is of the form I_zN_z, while the water magnetization is along the y axis. The selective water pulse at this point rotates the water signal to the –z axis, followed by the application of a gradient g3 to minimize radiation damping. Subsequently, ^{15}N magnetization evolves during the t_1 delay ($t_1 = t_1^a + t_1^b - \tau_b$), with refocusing of antiphase magnetization occurring for a duration of $\tau_b + t_1^a - t_1^b = 1/(2J_{NH})$, so that at point b in the
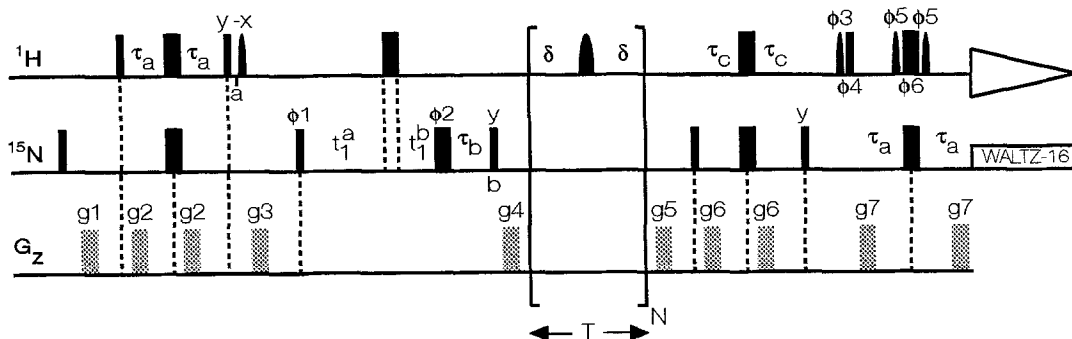
Fig. 1. Pulse sequence for the simultaneous measurement of longitudinal ^{15}N decay rates and chemical exchange rates. Narrow and wide pulses indicate 90° and 180° pulses, respectively and, unless indicated otherwise, all pulses are applied along the x-axis. The value of τ_a was set to 2.25 ms ($< 1/(4J_{NH})$), $t_1^a = \tau_c + t_1/2$, $t_1^b = t_1/2 - n\zeta$, $\tau_b = \tau_c - n\zeta$, $\delta = 2.5$ ms. The delay τ_c was set to 2.75 ms ($1/(4J_{NH})$), $\zeta = \tau_c/(N - 1)$, where N is the number of complex points in the nitrogen dimension, n = 0,1,2..., (N − 1), and t_1 is given by the relation $t_1 = n/SW1$, where SW1 is the spectral width in F_1 (Grzesiek and Bax, 1993b; Logan et al., 1993). WALTZ-16 decoupling (Shaka et al., 1983) of ^{15}N during acquisition was achieved using a 1 kHz field. The 90° water selective pulses are applied with the carrier on the water resonance, using either a 2 ms SEDUCE-1 pulse (~ 270 Hz field at peak height) (McCoy and Mueller, 1992) or a 125 Hz rectangular pulse. The 180° ^{1}H pulses applied during the mixing period T are applied as 550 μs cosine-modulated pulses (Smallcombe, 1993) with an excitation maximum 2 kHz from the water resonance frequency. A relaxation delay of 1 s is employed for all experiments, with the exception of the fully relaxed experiment performed to measure equilibrium constants, where a relaxation delay of 5 s was used. Phase cycling used for the experiments is: $\phi1 = x$; $\phi2 = 4(x),4(y),4(-x),4(-y)$; $\phi3 = 2(x),2(-x)$; $\phi4 = 2(x),2(-x)$; $\phi5 = x,-x$; $\phi6 = -x,x$ and receiver $2(x),4(-x),2(x)$. Quadrature in F_1 is achieved via States-TPPI of $\phi1$ (Marion et al., 1989). The gradient durations and levels are as follows: g1 = 1 ms, 5 G cm^{-1}; g2 = 0.5 ms, 4 G cm^{-1}; g3 = 1 ms, 15 G cm^{-1}; g4 = 1 ms, −20 G cm^{-1}; g5 = 0.5 ms, −10 G cm^{-1}; g6 = 0.5 ms, 8 G cm^{-1}; g7 = 0.125 ms, 25 G cm^{-1}. A delay of at least 50 μs is inserted between all gradients and subsequent rf pulses.

sequence the signal is in-phase. Note that the ^{1}H 180° pulse applied during this period rotates the water magnetization, so that it is aligned along the +z axis. The ^{15}N 90_y pulse at point b establishes z nitrogen magnetization, which is allowed to relax/exchange during the mixing time T. The pulse scheme that we employ is not of the enhanced-sensitivity type (Cavanagh et al., 1991; Palmer et al., 1991b), since ^{15}N magnetization is recorded prior to the T period and it is not possible to preserve both cosine- and sine-modulated t_1 components during this time. In order to minimize water saturation, caused by application of ^{1}H 180° pulses every few milliseconds during T, these pulses are applied as cosine-modulated pulses (Smallcombe, 1993) which have a broad excitation null on resonance (i.e., on the water). Controls using the SH3 sample have shown that for T values used in the experiment, ranging from 10 to 850 ms, the application of such selective pulses did not increase the level of water saturation. After the T period, magnetization is returned to the NH proton for detection via an INEPT pulse scheme (Morris and Freeman, 1979). During the $2\tau_c$ period the water magnetization is inverted, so that it is aligned along the −z axis. However, the combined action of the selective water pulse of phase $\phi3$ and the hard ^{1}H 90° pulse of phase $\phi4$ ensures that the water magnetization is restored to the +z axis. The final ^{1}H 180° pulse of phase $\phi6$ is surrounded by water-selective 90° pulses of phase $\phi5$ and pulsed field gradients g7 (Piotto et al., 1992). This ensures that the water magnetization is along the +z axis immediately prior to the detection period.

In order to evaluate the exchange rates, spectra are collected for a range of mixing times, and

peak volumes are used to characterize the decay/buildup curves of the magnetization as it evolves during the mixing period. It is straightforward to calculate the solution of the Bloch equations for a system undergoing chemical exchange between two sites (Hahn and Maxwell, 1952; Gutowsky et al., 1953; McConnell, 1958; Hull and Sykes, 1975). In this derivation we note that in the sequence of Fig. 1 phase cycling of the ^{15}N 180° pulse of phase $\phi2$ ensures that ^{15}N magnetization is placed alternatively along the $+z$ and $-z$ axes, so that, averaged over the complete phase cycle of $\phi2$, the evolution of $I_{nn}(T)$ and $I_{uu}(T)$ does not depend on the values of $I_n(\infty)$ and $I_u(\infty)$ (Sklenar et al., 1987). The intensities of the auto peaks for the two states denoted by 'n' and 'u' are then given by

$$I_{nn}(T) = I_n(0) \, (-(\lambda_2 - a_{11}) \, e^{-\lambda_1 T} + (\lambda_1 - a_{11}) \, e^{-\lambda_2 T})/(\lambda_1 - \lambda_2) \tag{1a}$$

$$I_{uu}(T) = I_u(0) \, (-(\lambda_2 - a_{22}) \, e^{-\lambda_1 T} + (\lambda_1 - a_{22}) \, e^{-\lambda_2 T})/(\lambda_1 - \lambda_2) \tag{1b}$$

while the intensities of the exchange peaks corresponding to the transfer of magnetization from 'n' to 'u' ($I_{nu}(T)$) and from 'u' to 'n' ($I_{un}(T)$) are given by

$$I_{nu}(T) = I_n(0) \, (a_{21} \, e^{-\lambda_1 T} - a_{21} \, e^{-\lambda_2 T})/(\lambda_1 - \lambda_2) \tag{1c}$$

and

$$I_{un}(T) = I_u(0) \, (a_{12} \, e^{-\lambda_1 T} - a_{12} \, e^{-\lambda_2 T})/(\lambda_1 - \lambda_2) \tag{1d}$$

respectively. In Eq. 1a–d, $\lambda_{1,2}$ is defined according to the relation $\lambda_{1,2} = 1/2\{(a_{11} + a_{22}) \pm [(a_{11} - a_{22})^2 + 4k_{nu}k_{un}]^{1/2}\}$, $a_{11} = R_n + k_{nu}$, $a_{12} = -k_{un}$, $a_{21} = -k_{nu}$, $a_{22} = R_u + k_{un}$, R_u and R_n are the longitudinal relaxation rates of magnetization in sites u and n, $I_n(0)$ and $I_u(0)$ denote the amount of longitudinal nitrogen magnetization associated with states n and u at the start of the mixing period T, and k_{nu} and k_{un} are the exchange rates for magnetization converting from site n to u and u to n, respectively. In the limit where $R_n = R_u$ and $k_{nu} = k_{un}$, Eq. 1 reduces to Eq. 9.1.5 in the text by Ernst et al. (1987).

A least-squares fitting procedure can be employed to extract the longitudinal decay and chemical exchange rates by fitting the expressions given in Eq. 1 to the measured intensities of auto and exchange peaks. The volumes of auto peaks from a separate data set, recorded under fully relaxed conditions with zero mixing time, provide a measure of the equilibrium constants at each site in the molecule, $K_{eq} = k_{un}/k_{nu}$, which we have used to constrain the relative values of k_{un} and k_{nu} obtained from Eq. 1. It is important to note that $K_{eq} = I_n(0)/I_u(0)$ only if spectra are acquired with sufficiently long relaxation delays to allow the full recovery of NH magnetization from states 'n' and 'u', and if losses during the INEPT transfers to and from ^{15}N magnetization are negligible. Similarly, these same conditions result in exchange peaks of equal intensity, i.e., $I_{nu}(T) = I_{un}(T)$.

Figure 2 contains a small region from a number of data sets, showing both auto and exchange peaks for Gly[46] in the N-terminal SH3 domain of drk. Delays of 11, 155 and 843 ms are shown. It is clear that the intensities of the auto peaks decrease with increasing T, while the exchange peaks increase to a maximum in intensity (at $T = (\lambda_2 - \lambda_1)^{-1} \ln(\lambda_2/\lambda_1)$) and subsequently decrease in intensity. Figure 3 shows the measured data points and the curves (Eq. 1) obtained from a

least-squares fitting procedure for Gly[46]. The longitudinal decay and exchange rates extracted from the data are: $R_n = 2.41 \pm 0.05$ s^{-1}, $R_u = 1.90 \pm 0.11$ s^{-1}, $k_{nu} = 0.43 \pm 0.03$ s^{-1}, $k_{un} = 0.86 \pm 0.06$ s^{-1}. In addition, values for $I_n(0)$ and $I_u(0)$ are also extracted from the fit. A Monte Carlo approach was used to estimate the errors in the rates extracted from the fit (Kamath and Shriver, 1989; Palmer et al., 1991a). Briefly, the uncertainties in the intensities of the measured data points comprising the $I_{nn}(T)$, $I_{uu}(T)$, I_{nu} (T) and $I_{un}(T)$ curves were estimated from the standard deviations of the residuals between the best fit curves and the measured data. One hundred simulated data sets were created from the addition of the appropriate random errors to the simulated curves derived from the best fit parameters. The simulated data sets were then subjected to the least-squares fitting procedure, parameters extracted and estimates of the errors of the fitting parameters obtained from the distribution of the parameters (assumed to be Gaussian). It is interesting to note that the best fit of the data places the exchange curve for 'u' to 'n' slightly above the exchange curve for the transfer from 'n' to 'u'. This is, at least in part, due to the fact that the NH T_1 values in the unfolded state are lower than in the folded state (in the case of Gly[46], 0.39 versus 0.73 s) and that fully relaxed spectra were not recorded. (This does not result in errors in the measured values, since the equilibrium constants used were obtained from fully relaxed spectra.) Since the intensities of $I_n(0)$ and $I_u(0)$ are directly related to the steady-state NH magnetization
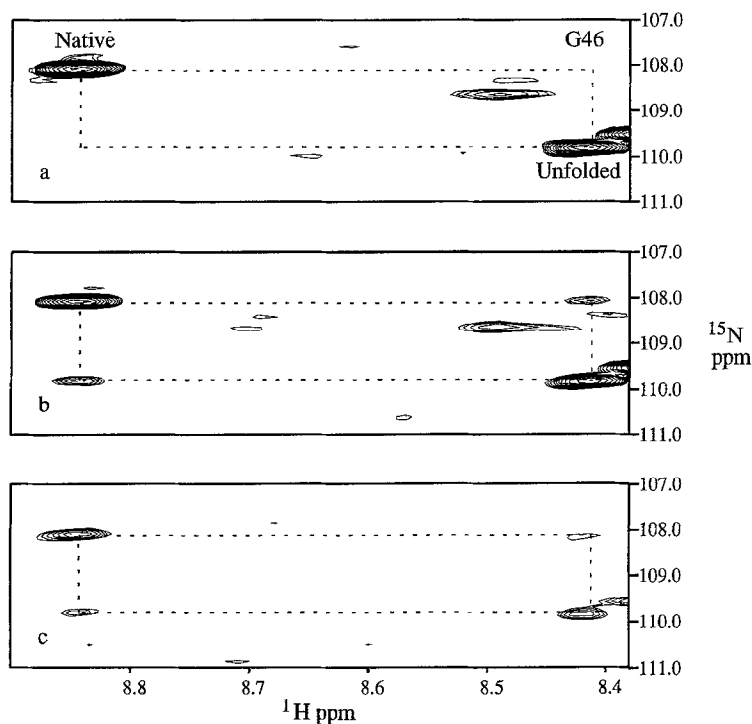

Fig. 2. Selected regions of spectra containing peaks of Gly[46] from the N-terminal SH3 domain of drk. Spectra were recorded on a Varian UNITY 500 MHz spectrometer, equipped with a pulsed field gradient unit and an actively shielded gradient probe. The sample concentration was 1.0 mM, pH 6.0, 50 mM sodium phosphate, 14 °C. The spectra correspond to the following delays T: (a) 0.011 s; (b) 0.155 s; and (c) 0.843 s. The peaks are labeled as described in the text.
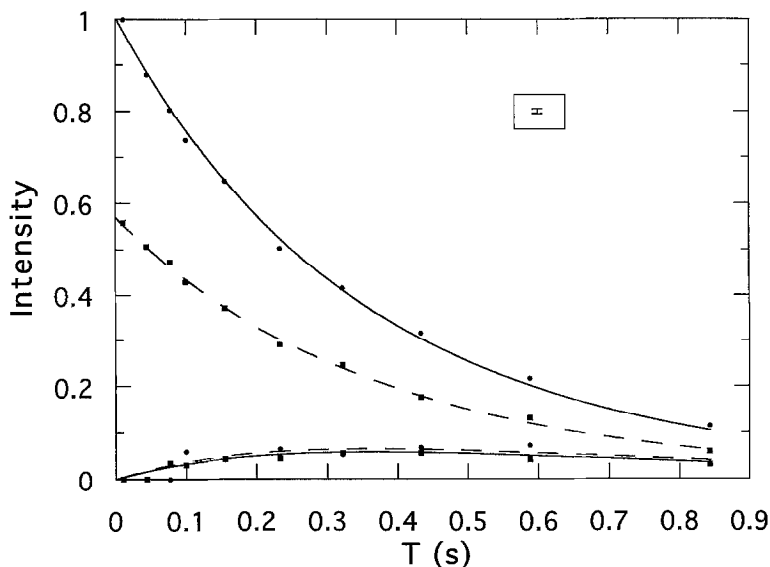
Fig. 3. Experimental data and fitted curves for Gly[46]. The upper two curves describe the decay of auto peaks, while the lower curves show the buildup/decay of the exchange peaks. Solid lines indicate the best fit curves for magnetization originating in the native state (i.e., $I_{nn}(t)$ and $I_{nu}(t)$) and broken lines indicate the best fit curves for magnetization originating in the unfolded state ($I_{uu}(t)$ and $I_{un}(t)$). Experimental data points are indicated with (●) for magnetization originating in the folded form and with (■) for magnetization originating in the unfolded form. In cases where it is not possible to extract the peak heights of the exchange peaks (for small values of T), these points are indicated as having zero intensity and were not used in the fitting process. A representative error bar for the fitted curves is shown in the upper right-hand corner.

values for residues in the native and unfolded states, respectively, the value of $I_n(0)$ will be preferentially decreased relative to $I_u(0)$ and $I_{nu}(T) < I_{un}(T)$ (see Eq. 1c,d).

It is instructive to compare the method described in the present paper with an approach which makes use of the exchange of two-spin order, I_zS_z ($I = {}^1H$, $S = {}^{15}N$ or ^{13}C), in order to extract rate constants for exchange processes. In the case of proteins and other large molecules, longitudinal two-spin order decays more efficiently than heteronuclear z magnetization, due to the presence of ^1H spin flips which can efficiently relax two-spin ^1H-S order. The increased relaxation rates of the auto peaks in the I_zS_z experiment result in exchange peaks with reduced signal in relation to the S_z experiment and in addition increase the lower bound of exchange rates that can be measured. Figure 4 illustrates the relative exchange peak intensities as a function of mixing time T for S_z versus I_zS_z exchange experiments for Gly[46], using measured values of relaxation times and exchange rates. In the derivation of the profile for the I_zS_z exchange experiment we have assumed that the relaxation of I_zS_z (neglecting exchange) can be described with a single exponential. In fact, all protons in proximity to the proton which participates in the two-spin order contribute to the relaxation of I_zS_z and the relaxation is almost certainly multiexponential. For this reason, exchange rates are often extracted from the initial buildup rate of exchange peaks in I_zS_z experiments (Otting et al., 1993). Unfortunately, such an approach is often limited by poor signal-to-noise ratios. Previous experiments attempting to characterize the exchange rate constants for the N-terminal SH3 domain of drk, based on exchange of two-spin order, provided only approximate
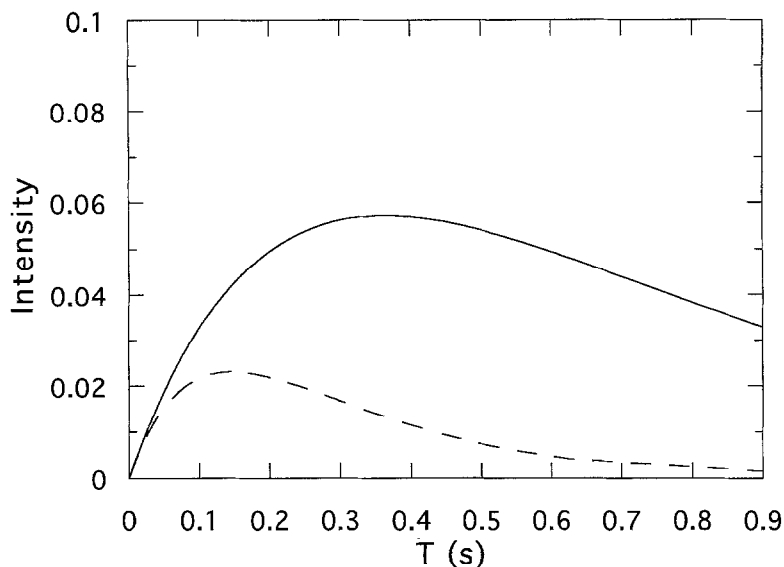
Fig. 4. Simulated exchange peak intensities as a function of mixing time, arising from exchange of S_z (solid line) and I_zS_z magnetization (dashed line) between two sites. The rates used in the simulations are taken from measured values for Gly[46] in the SH3 fragment. The S_z and I_zS_z decay rates used are 2.41 s^{-1} (1.90 s^{-1}) and 8.03 s^{-1} (4.58 s^{-1}) respectively, for folded (unfolded) states; $k_{un} = 0.86$ s^{-1}; $k_{nu} = 0.43$ s^{-1}.

rates of exchange. Figure 4 indicates clearly that the exchange peaks are much more intense in the S_z exchange experiment relative to the I_zS_z experiment and that slower exchange rates can be measured.

In summary, in this communication we have described an approach for the accurate determination of both chemical exchange and longitudinal decay rates. Care has been taken to avoid water saturation, so that complicating effects introduced by NH exchange with water are minimal.

ACKNOWLEDGEMENTS

REFERENCES

Bax, A. and Davis, D. (1985) *J. Magn. Reson.*, **63**, 207–213.
Bax, A. and Pochapsky, S. (1992) *J. Magn. Reson.*, **99**, 638–643.
Bothner-By, A.A., Stephens, R.L., Lee, J., Warren, C.D. and Jeanloz, R.W. (1984) *J. Am. Chem. Soc.*, **106**, 811–813.
Boyd, J., Hommel, U. and Campbell, I.D. (1990) *Chem. Phys. Lett.*, **175**, 477–482.
Cavanagh, J., Palmer, A.G., Wright, P.E. and Rance, M. (1991) *J. Magn. Reson.*, **91**, 429–435.

Ernst, R.R., Bodenhausen, G. and Wokaun, A. (1987) *Principles of Nuclear Magnetic Resonance in One and Two Dimensions*, Clarendon Press, Oxford, p. 492.

Forsen, S. and Hoffman, R.A. (1963) *J. Chem. Phys.*, **39**, 2892–2901.

Grzesiek, S. and Bax, A. (1993a) *J. Am. Chem. Soc.*, **115**, 12593–12594.

Grzesiek, S. and Bax, A. (1993b) *J. Biomol. NMR*, **3**, 185–204.

Gutowsky, H.S., McCall, D.W. and Slichter, C.P. (1953) *J. Chem. Phys.*, **21**, 279–292.

Gutowsky, H.S. and Saika, A. (1953) *J. Chem. Phys.*, **21**, 1688–1694.

Hahn, E.L. and Maxwell, D.E. (1952) *Phys. Rev.*, **88**, 1070–1084.

Hull, W.E. and Sykes, B.D. (1975) *J. Chem. Phys.*, **63**, 867–880.

John, B.K., Plant, D., Webb, P. and Hurd, R.E. (1992) *J. Magn. Reson.*, **98**, 200–206.

Kamath, U. and Shriver, J.W. (1989) *J. Biol. Chem.*, **264**, 5586–5592.

Kay, L.E., Torchia, D.A. and Bax, A. (1989) *Biochemistry*, **28**, 8972–8979.

Kay, L.E., Nicholson, L.K., Delaglio, F., Bax, A. and Torchia, D.A. (1992) *J. Magn. Reson.*, **97**, 359–375.

Kay, L.E., Xu, G.Y. and Yamazaki, T. (1994) *J. Magn. Reson. Ser. A*, in press.

Logan, T.M., Olejniczak, E.T., Xu, R.X. and Fesik, S.W. (1993) *J. Biomol. NMR*, **3**, 225–231.

Macura, S. and Ernst, R.R. (1980) *Mol. Phys.*, **41**, 95–117.

Marion, D., Ikura, M., Tschudin, R. and Bax, A. (1989) *J. Magn. Reson.*, **85**, 393–399.

McConnell, H.M. (1958) *J. Chem. Phys.*, **28**, 430–431.

McCoy, M. and Mueller, L. (1992) *J. Am. Chem. Soc.*, **114**, 2108–2112.

Montelione, G.T. and Wagner, G. (1989) *J. Am. Chem. Soc.*, **111**, 3096–3098.

Morris, G.A. and Freeman, R. (1979) *J. Am. Chem. Soc.*, **101**, 760–762.

Otting, G., Liepinsh, E. and Wüthrich, K. (1993) *Biochemistry*, **32**, 3571–3582.

Palmer III, A.G., Rance, M. and Wright, P.E. (1991a) *J. Am. Chem. Soc.*, **113**, 4371–4380.

Palmer III, A.G., Cavanagh, J., Wright, P.E. and Rance, M. (1991b) *J. Magn. Reson.*, **93**, 151–170.

Palmer III, A.G., Skelton, N.J., Chazin, W.J., Wright, P.E. and Rance, M. (1992) *Mol. Phys.*, **75**, 699–711.

Piotto, M., Saudek, V. and Sklenar, V. (1992) *J. Biomol. NMR*, **2**, 661–665.

Shaka, A.J., Keeler, J., Frenkiel, T. and Freeman, R. (1983) *J. Magn. Reson.*, **52**, 335–338.

Sklenar, V., Torchia, D.A. and Bax, A. (1987) *J. Magn. Reson.*, **73**, 375–379.

Smallcombe, S. (1993) *J. Am. Chem. Soc.*, **15**, 4776–4785.

Wider, G., Neri, D. and Wüthrich, K. (1991) *J. Biomol. NMR*, **1**, 93–98.

Zhang, O. and Forman-Kay, J.D. (1994) *Biochemistry*, submitted for publication.